

# Simulating the Double Slit Experiment with the Crank-Nicolson Scheme.

Sigurd S. Vargdal, Brage A. Trefjord, Nils E. C. Taugbøl and Frida O. Sørensen\*

*University of Oslo, Department of Physics*

(Dated: January 13, 2023)

Quantum mechanics is governed by the Schrödinger equation, a partial differential equation (PDE) that involves time- and spacial-derivatives. The double-slit experiment using particles is one of the fundamental experiments underlying quantum mechanics. We therefore simulate the double-slit experiment applying the Crank-Nicolson scheme to solve the Schrödinger equation, and evaluate the results. We find that the deviation of the total probability is of order  $10^{-15}$ . As we calculate the probability with 64-bit floating point numbers, this is close to the precision that the computer can handle. The interference patterns of the probability density are identical to the results of the double-slit experiments, making the Crank-Nicolson scheme a well-suited method for solving the Schrödinger equation.

## I. INTRODUCTION

The discovery of quantum mechanics has revolutionised modern physics and the way we understand the universe. One of the most important experiments for the formulation of quantum mechanics is the double-slit experiment, which proved that particles can have wave-like properties. The experiment consists in sending particles through a barrier with two openings, slits, and measuring where the particles end up by use of a detector set at a fixed distance behind the slits. It illustrates the wave-like properties of the particles as they interact with themselves, creating interference patterns on the detector as it evolves forward in time. An example of the interference of a plane wave propagating through a double slit is illustrated in Figure 1, which corresponds well with double slit experiments using particles [1].

This leads us to interpret matter particles as having wave-like properties and to another important result in quantum mechanics, the Schrödinger equation.

The Schrödinger equation was published by Erwin Schrödinger in 1926 [2] and governs the evolution of the wave equation. It won him the Nobel Prize in Physics along with Paul Adrien Maurice Dirac in 1933 [3]. The Schrödinger equation is a partial differential equation (PDE) which we will use to simulate the double-slit experiment using a numerical approach, namely the Crank-Nicolson scheme. In this report we study how well the Crank-Nicolson scheme is suited to simulate the evolution of the Schrödinger equation through a double slit.

The report is structured as follows. In section II we begin by laying out the necessary background in quantum mechanics followed by the setup of the simulation.

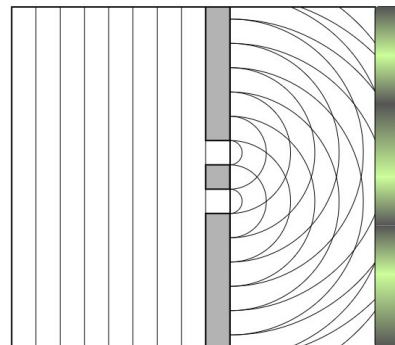


Figure 1: Sketch of the double slit experiment with a plane wave. The amplitude of the interference pattern should reduce as the distance from the center increases on the detection wall.

Thereafter we introduce notation and set up the Crank-Nicolson scheme. Then, in section III we lay out the results of our simulations. In section IV we discuss our results and findings. We also discuss possibilities for future work. Lastly in section V we sum up our conclusions.

---

\* Repository:

[https://github.com/NilsECT/FYS3150/tree/main/Project\\_5/](https://github.com/NilsECT/FYS3150/tree/main/Project_5/)

## II. METHOD

### A. The double-slit experiment

#### 1. The Schrödinger equation

The Schrödinger equation

$$i\hbar \frac{d}{dt} |\Psi\rangle = \hat{H} |\Psi\rangle. \quad (1)$$

tells us how a quantum state, a complex vector in Hilbert space denoted by  $|\Psi\rangle$ , evolves in time. The Hamiltonian  $\hat{H}$  describes the system with a kinetic and potential term,  $i$  is the complex number  $\sqrt{-1}$ , and  $\hbar$  is the reduced Planck constant. We will not impose any interpretation of quantum mechanics and so what the quantum state *is* is left for the reader to interpret. We must however agree that the quantum state fully describes a system/object at a specific instance in time. In this report we will consider the quantum state to fully describe a single particle.

We will also consider the position representation of the state in two dimensions, meaning we will represent the state as a wave function  $\langle x, y | \Psi \rangle = \Psi(x, y, t)$ . We will not consider relativistic particles so we can express (1) as

$$i\hbar \frac{\partial}{\partial t} \Psi(x, y, t) = -\frac{\hbar^2}{2m} \left( \frac{\partial^2}{\partial x^2} + \frac{\partial^2}{\partial y^2} \right) \Psi(x, y, t) + V(x, y, t) \Psi(x, y, t). \quad (2)$$

The double partial derivatives here are the kinetic terms for both spatial dimensions, and we set the potential  $V(x, y, t)$  as time independent  $V(x, y, t) = V(x, y)$ .

We consider the wave function to contain probabilities for every possible measurable position. The probability density of the particle's position can be found through the Born rule. The Born rule is given by

$$p(x, y, t) = |\Psi(x, y, t)|^2 = \Psi^*(x, y, t) \Psi(x, y, t).$$

Here,  $p$  is the probability of finding the particle at a point  $(x, y)$  at a time  $t$ . The probability to find the particle anywhere has to be 1 as the particle has to be located somewhere. This implies that in order to apply the Born rule, the wave function must be normalised.

We reduce (2) to be dimensionless and set  $x, y \in [0, 1]$ , and  $t \in [0, T]$ , where  $T$  is the total time. Further, we define the dimensionless wave function as  $u(x, y, t)$  which gives rise to the following simplified expression for equation (2);

$$i \frac{\partial u(x, y, t)}{\partial t} = - \left( \frac{\partial^2}{\partial x^2} + \frac{\partial^2}{\partial y^2} + V(x, y) \right) u(x, y, t), \quad (3)$$

where  $u(x, y, t)$  is normalised.

#### 2. Experiment

We set up the initial wave function as an unnormalised Gaussian wave packet

$$u(x, y, t = 0) = e^{-\frac{(x-x_c)^2}{2\sigma_x^2} - \frac{(y-y_c)^2}{2\sigma_y^2} + ip_x(x-x_c) + ip_y(y-y_c)}$$

where  $x_c$  and  $y_c$  denote the coordinates of the centre of the wave packet,  $\sigma_x$  and  $\sigma_y$  are the standard deviations of the wave packet in their respective directions, and  $p_x$  and  $p_y$  are the momenta of the wave packet in each direction. The double-slit will be simulated by placing a large potential  $v_0 \gg 1$  as a wall centered around  $x = 0.5$ , with a thickness of  $\Delta x = 0.02$ . The slits will be centered around  $y = 0.5$  with apertures of  $\Delta y_{\text{aperture}} = 0.05$  with a distance  $\Delta y = 0.05$  between each slit. At the apertures, the potential is zero. To normalise  $u(x, y, t)$  we impose the condition that

$$\sum_{x, y} u(x, y, 0)^* u(x, y, 0) = 1.$$

This is the probability of finding the particle anywhere in the system and has to be conserved over time.

Moreover, quantum mechanics requires the wave function to vanish at infinity, meaning it converges to zero as  $x, y \rightarrow \infty$ . To avoid having to consider infinity in our simulation, we impose Dirichlet boundary conditions. This means that we set

$$u(x, y, t) = 0, \quad \forall x, y \in \{0, 1\},$$

meaning that the wave function is zero at the boundary. This ensures that we fulfil the requirement that the wave function vanishes at infinity.

### B. Numerical approach

#### 1. Notation and discretisation

Before delving into the methods we will use to simulate the double-slit experiment, we introduce some new notation along with a discretisation of the system. The partial differential equation which we seek to solve is 2+1-dimensional, since it has two dimensions in space and one dimension in time. We discretise both spatial dimensions equally by dividing their domain into  $M$  points with constant step size  $h$ . We can now express the  $x$  and  $y$  coordinates as

$$x_i = ih, \quad i \in \{0, 1, 2, \dots, M-1\}$$

$$y_j = jh, \quad j \in \{0, 1, 2, \dots, M-1\},$$

where  $i$  and  $j$  are real integers. This discretisation of the spacial dimensions defines the grid on which we will simulate the double-slit experiment. The imposed Dirichlet boundary conditions allow us to omit  $i, j = \{0, M\}$

when setting up the numerical scheme as the value at those points will always be 0. Thus we can rewrite the domains of  $i$  and  $j$  as

$$\begin{aligned} i &\in \{1, 2, \dots, M-2\} \\ j &\in \{1, 2, \dots, M-2\}. \end{aligned}$$

Similarly, we discretise the dimension in time into  $N_t$  points with a time step  $\Delta t$ . We write the discretised time as

$$t_n = n\Delta t, n \in \{0, 1, 2, \dots, N_t\}.$$

A point  $u(x_i, y_j, t_n)$  can then be expressed as  $u_{i,j}^n$ , and the discretised potential can be written as  $V(x_i, y_j) \rightarrow v_{i,j}$ . By discretising the wave function  $u_{i,j}^n$ , the probability density  $p(x, y; t)$  simply becomes the probability for the particle to be located at the tile corresponding to  $(x_i, y_j)$  in the discretised grid. This probability can be calculated from

$$P(x_i, y_j; t) = u_{i,j}^{n*} u_{i,j}^n.$$

where  $u_{i,j}^{n*}$  denotes the complex-conjugate of  $u_{i,j}^n$ .

## 2. The Crank-Nicolson scheme

The Crank-Nicolson scheme is a linear combination of the forward difference and backward difference methods for solving partial differential equations. Therefore, we give a short presentation of both aforementioned methods. We start by representing the right hand side of (3) as  $F(x, y, t)$ , such that

$$F_{i,j}^n \equiv - \left( \frac{\partial^2}{\partial x^2} - \frac{\partial^2}{\partial y^2} \right) u_{i,j}^n + v(x, y) u_{i,j}^n.$$

The forward difference method approximates (3) as

$$i \frac{u_{i,j}^{n+1} - u_{i,j}^n}{\Delta t} = F_{i,j}^n,$$

where we truncate the local error  $\mathcal{O}(\Delta t)$  and

$$\begin{aligned} F_{i,j}^n &= - \frac{u_{i+1,j}^n - 2u_{i,j}^n + u_{i-1,j}^n}{h^2} \\ &\quad - \frac{u_{i,j+1}^n - 2u_{i,j}^n + u_{i,j-1}^n}{h^2} \\ &\quad + v_{i,j} u_{i,j}^n. \end{aligned}$$

We note that the forward difference method is explicit as it only requires the solution of  $F$  at the current time step  $n$ . The backward difference method approximates (3) as

$$i \frac{u_{i,j}^{n+1} - u_{i,j}^n}{\Delta t} = F_{i,j}^{n+1},$$

where we again truncate away the same local error and

$$\begin{aligned} F_{i,j}^{n+1} &= - \frac{u_{i+1,j}^{n+1} - 2u_{i,j}^{n+1} + u_{i-1,j}^{n+1}}{h^2} \\ &\quad - \frac{u_{i,j+1}^{n+1} - 2u_{i,j}^{n+1} + u_{i,j-1}^{n+1}}{h^2} \\ &\quad + v_{i,j} u_{i,j}^{n+1}. \end{aligned}$$

As opposed to the forward difference method, the backward difference method requires the solution of  $F$  at the next time step  $n+1$ . This requires us to solve a set of equations to find the six unknowns and is therefore an implicit method.

The Crank-Nicolson scheme combines the forward difference and backward difference methods as

$$i \frac{u_{i,j}^{n+1} - u_{i,j}^n}{\Delta t} = \frac{1}{2} (F_{i,j}^n + F_{i,j}^{n+1}),$$

where we combine the forward and backward difference methods equally weighted. By inserting the expressions for  $F_{i,j}^n$  and  $F_{i,j}^{n+1}$ , moving all the  $n+1$  terms to the left hand side, and moving all the  $n$  terms to the right hand side, we get

$$\begin{aligned} &u_{i,j}^{n+1} - r [u_{i+1,j}^{n+1} - 2u_{i,j}^{n+1} + u_{i-1,j}^{n+1}] - r [u_{i,j+1}^{n+1} \\ &\quad - 2u_{i,j}^{n+1} + u_{i,j-1}^{n+1}] + \frac{i\Delta t}{2} v_{i,j} u_{i,j}^{n+1} \\ &= u_{i,j}^n + r [u_{i+1,j}^n - 2u_{i,j}^n + u_{i-1,j}^n] \\ &\quad + r [u_{i,j+1}^n - 2u_{i,j}^n + u_{i,j-1}^n] - \frac{i\Delta t}{2} v_{i,j} u_{i,j}^n, \end{aligned} \quad (4)$$

where  $r \equiv \frac{i\Delta t}{2h^2}$ . We have included the full derivation of (4) in appendix A.

We can write (4) explicitly as a matrix equation

$$A \mathbf{u}^{n+1} = B \mathbf{u}^n,$$

where the vector  $\mathbf{u}^n$  contain all  $(M-2)^2$  points  $u_{i,j}$  at a time step  $n$  as

$$\begin{aligned} \mathbf{u}^n &= [(u_{1,1}^n, u_{2,1}^n, \dots, u_{M-2,1}^n), \\ &\quad (u_{1,2}^n, \dots, u_{M-2,2}^n), \\ &\quad \dots, \\ &\quad (u_{1,M-2}^n, \dots, u_{M-2,M-2}^n)]. \end{aligned}$$

The matrices  $A$  and  $B$  are tridiagonal  $(M-2)^2 \times (M-2)^2$  matrices

$$A = \begin{bmatrix} A_{k=1} & D(-r) & 0 & 0 \\ D(-r) & A_{k=2} & \ddots & 0 \\ 0 & \ddots & \ddots & D(-r) \\ 0 & 0 & D(-r) & A_{k=M-2} \end{bmatrix},$$

and

$$B = \begin{bmatrix} B_{k=1} & D(r) & 0 & 0 \\ D(r) & B_{k=2} & \ddots & 0 \\ 0 & \ddots & \ddots & D(r) \\ 0 & 0 & D(r) & B_{k=M-2} \end{bmatrix},$$

where  $D(r)$  are  $(M-2) \times (M-2)$  diagonal matrices with  $r$  along their diagonals. The submatrices along the diagonal of  $A$  are

$$A_k = \begin{bmatrix} a_k & -r & & 0 \\ -r & a_{2k} & \ddots & \\ & \ddots & \ddots & -r \\ 0 & & -r & a_{(M-2)k} \end{bmatrix},$$

and along the diagonal of  $B$  the submatrices are

$$B_k = \begin{bmatrix} b_k & r & & 0 \\ r & b_{2k} & \ddots & \\ & \ddots & \ddots & r \\ 0 & & r & b_{(M-2)k} \end{bmatrix}.$$

The indices of these submatrices are  $k \in \{1, 2, \dots, M-2\}$ . The entries  $a_g$  and  $b_g$  have indices that correspond to a matrix index  $(i, j)$  from  $u_{i,j}^n$  where

$$g = i + j(M-2),$$

and the values assigned to each entry is

$$a_g = 1 + 4r + \frac{i\Delta t}{2}v_{ij},$$

$$b_g = 1 - 4r - \frac{i\Delta t}{2}v_{ij}.$$

When  $i$  is not used as an index, it denotes the complex number.

With this matrix representation of the Crank-Nicolson scheme, finding  $\mathbf{u}^{n+1}$  becomes straightforward. We compute  $\mathbf{b} = B\mathbf{u}^n$  and solve  $A\mathbf{u}^{n+1} = \mathbf{b}$  for  $\mathbf{u}^{n+1}$ . An outline of the algorithm for the Crank-Nicolson scheme can be found in Algorithm 1. The Crank-Nicolson scheme is stable for all choices of  $\Delta t$  and  $h$ , though it may, for some choices of time steps, show oscillatory errors that slowly converge [4].

### III. RESULTS

To evaluate the Crank-Nicolson scheme we first looked at how the total probability of the wave-packet evolved over time. Figure 2 shows the absolute difference between the total probability  $p(x, y)$  of the simulated wave-packet and the expected total probability, 1.

---

#### Algorithm 1: The Crank-Nicolson scheme:

---

```

 $\mathbf{u}^0$        $\triangleright$  Set and store initial conditions;
 $V$          $\triangleright$  Set up potential;
 $dt, h$      $\triangleright$  Set step size for time and space dimensions;
 $A, B$       $\triangleright$  Calculate  $A$  and  $B$  matrices;
for number of time steps do
     $\mathbf{b} = B\mathbf{u}^n$        $\triangleright$  Compute  $\mathbf{b}$ ;
     $A\mathbf{u}^{n+1} = \mathbf{b}$    $\triangleright$  Solve matrix equation for  $\mathbf{u}^{n+1}$ ;
    store new  $\mathbf{u}^{n+1}$ 
end

```

---

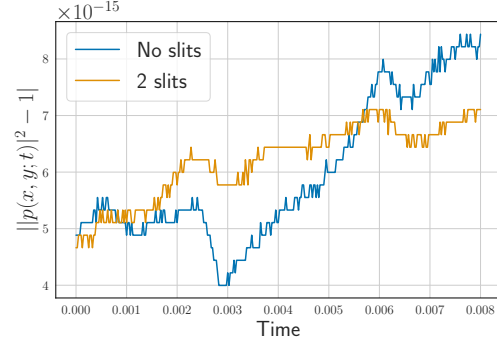


Figure 2: Deviation of the total probability from 1 at different times in the simulation. The blue graph is measured for an experiment with no barriers. The orange graph is obtained using a double-slit with  $\sigma_y = 0.10$ , and a potential of  $v_0 = 1 \times 10^{10}$ .

In the simulation with no potential barrier (labelled “no slit”), we used a time step  $\Delta t = 2.5 \times 10^{-5}$ , total time  $T = 0.008$ , and spatial step size  $h = 0.005$ . The Gaussian wave packet had initial parameters  $x_c = 0.25$ ,  $\sigma_x = 0.05$ ,  $p_x = 200$ ,  $y_c = 0.5$ ,  $\sigma_y = 0.05$ , and  $p_y = 0$ . In the same figure we have included the same type of deviation in a simulation with a potential barrier set up as a double-slit with a Gaussian wave packet of similar initial parameters, except we have set  $\sigma_y = 0.10$ . The potential strength was  $v_0 = 1 \times 10^{10}$ . We then proceeded to look at the probability distributions for finding the particle along the  $y$ -axis at  $x = 0.8$  and  $t = 0.002$  for different numbers of slits, namely 1, 2 and 3 slits, generated by the same potential  $v_0 = 1 \times 10^{10}$ . These probability distributions can be seen in Figure 3.

A few select frames of the double-slit simulation are shown in Figure 4a. The different times  $t \in \{0, 0.001, 0.002\}$  correspond respectively to the initial condition, the wave-packet reaching the slits and the wave packet after having passed through the double-slit. In Figures 4b and 4c we show the real and imaginary parts of the wave function for the same selected timestamps.

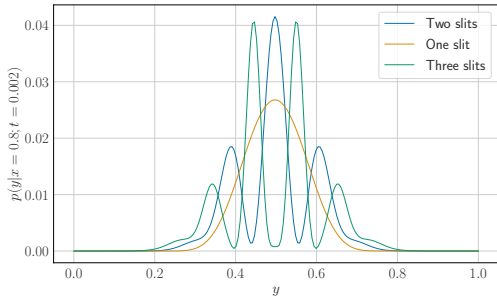


Figure 3: Probability along the  $y$ -axis given that the particle has hit a detection screen at  $x = 0.8$ , at time  $t = 0.002$ . Different graphs show the probability for different numbers of slits.

#### IV. DISCUSSION

Figure 2 shows how the total probability of the wave function evolves relative to the expected total probability 1. The total probability of the wave function when simulated without any potential barriers show a slight deviation from the expected total probability, after  $t \approx 0.002$ . This change is small, in the order  $10^{-15}$ . At the same time  $t \approx 0.002$ , when simulating with a double-slit, the difference shows an oscillatory motion after the wave packet has passed through the double-slit. At that time the wave function reaches the boundaries of the simulation and is reflected.<sup>1</sup> However, we can see that despite this slight oscillation in total probability, the wave function remains normalised. These changes are also in the order  $10^{-15}$ . This change is in the range of our numerical precision, as the computer can only represent numbers with a certain accuracy, and is therefore prone to errors when calculating around its floating point precision of 16 decimals [5]. It therefore seems likely that the deviation showed in Figure 2 is simply a lack of precision in the computer. The simulations can be regarded as reliable as the probabilistic properties of our simulations are conserved.

In Figure 4a we see how the wave function's behaviour evolve from three distinct timestamps for the modulus, real and imaginary part of the wave function. The timestamps are the initial position at  $t = 0$ , the time-point where the wave function reaches the double-slit at  $t = 0.001$  and the resulting wave function after having interacted with the double-slit at  $t = 0.002$ . It is clear that the potential acts as a barrier with a double-slit,

as expected. Part of the wave is reflected by the potential, and another part moves through the slits. The barrier is clearly visible at  $t = 0.001$ , where the  $u$ -values abruptly decrease to zero. At  $t = 0.002$  we can see the interference pattern of the probability density in Figure 4, which is in contrast to the straight path one would expect particles to take. We expected this kind of behaviour from a wave interfering with itself due to obstacles in its environment. As we have established in I, this is the result of the particle-wave duality. What we see is the particle interacting with itself. Figures 4b and 4c show the real and imaginary parts of the wave function respectively. The real part of the wave function equate to a cosine and the imaginary part of the wave equate to a sine. Together, they make up the modulus squared of the wave function, which is the calculated probability. The imaginary and real parts show a similar behavior, except with opposite phases that cancels when the modulus is computed.

The physical interpretation of the double slit experiment is that the probability density of the particle's position disappears once a measurement is taken as the wave function “collapses” and we know with certainty where the particle is. In our simulation we do not perform any measurement, rather, we observe how the probability of the particle's position evolves as it interacts with a double-slit. As we have imposed Dirichlet boundary conditions, the wave packet reaches the boundaries and is reflected back towards the double-slit. This is not a part of the double-slit experiment. Instead, it is a consequence of the boundary conditions we have chosen to use.

Figure 3 shows the probability distribution of the particle's position along the  $y$ -axis at  $x = 0.8$  and  $t = 0.002$ . The distributions' numbers of peaks varies together with the number of slits, where we have one peak for a single slit, three peaks for two slits and four

<sup>1</sup> An animation of the simulation with two slits can be found in the repository at [https://github.com/NilsECT/FYS3150/tree/main/Project\\_5/code/](https://github.com/NilsECT/FYS3150/tree/main/Project_5/code/), with the name “animation.mp4”.

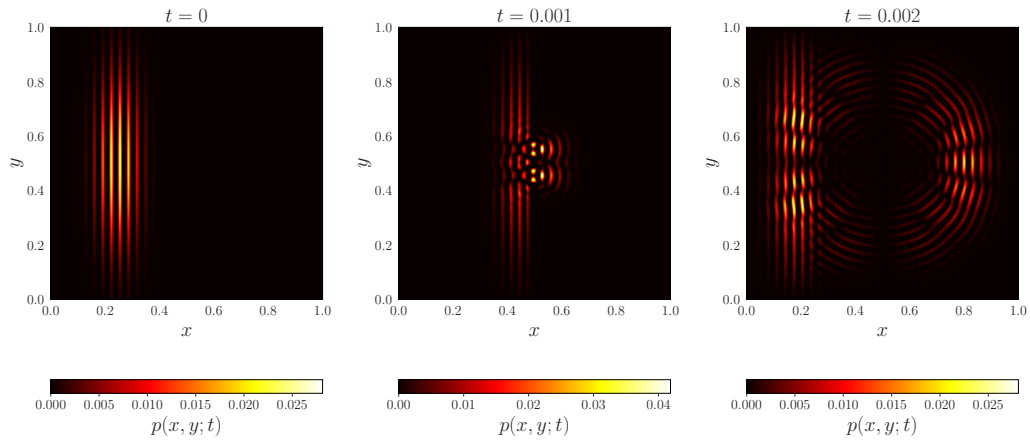
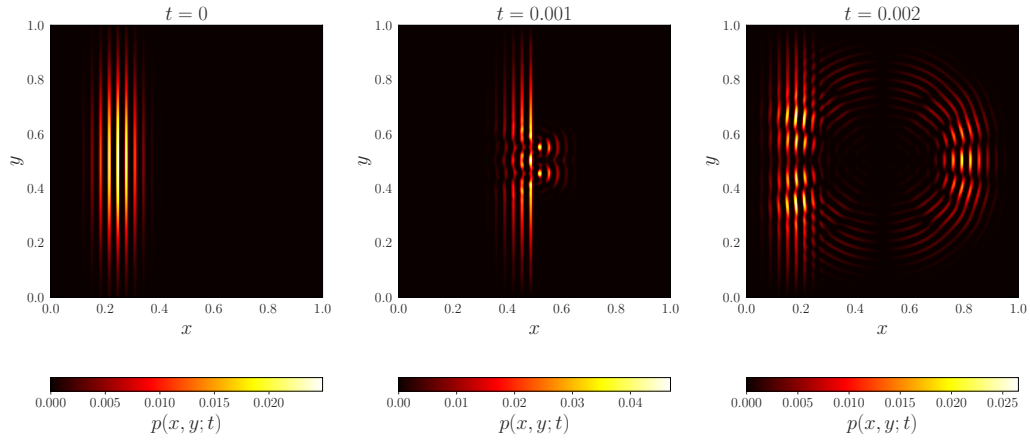
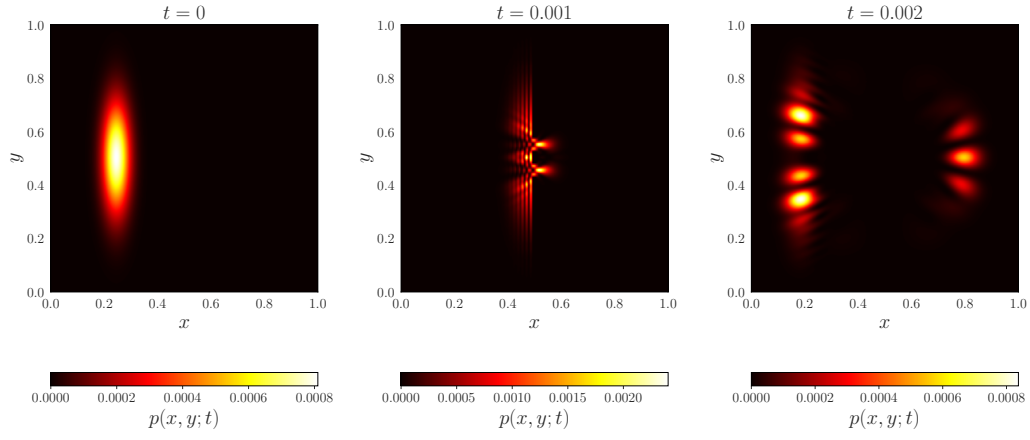


Figure 4: Probability of measuring the particle at different positions in the box, at three different times  $t = 0, 0.001, 0.002$ .



peaks for three slits. These patterns are also symmetric on  $y = 0.5$  and are identical to interference patterns of a wave. The probability distribution corresponds to the interference pattern of the double-slit experiment, and its variations, performed with particles that interact with themselves. The probability distribution along a would-be detection screen is identical to the results of the same experiment performed with particles [1]. This points again toward the wave-particle duality that lies as a foundation for quantum mechanics. We can also see in the rightmost figure in Figure 4a that the intensity of the probability is indeed highest at  $y = 0.5$  for a double-slit, which corresponds well with Figure 3.

#### A. Future work

We have looked at the experiment with one, two and three slits. This could be taken a step further to explore the computational limits of the model by increasing the number of slits. As the model is reliable, it could be used to study quantum tunnelling, that is, the wave function's ability to have non-zero values inside a potential. It could also be interesting to study this effect by reducing the potential of the wall, and look at how part of the wave might propagate through it.

We have exclusively looked at a closed system, as dictated by the Dirichlet boundary conditions. It would therefore have been interesting to look at the case with open boundaries so the wave could (in theory) propagate towards infinity.

As the model is reliable for the development of the wave function we could seek to introduce simulations of measurements. This could imply introducing

stochasticity to the model as well as more advanced quantum mechanics related theory. The basis of the evolution of the wave function is given here in this report and so introducing the possibility of taking measurements would only require to create a numerical measurement mechanism.

Lastly we could compare the Crank-Nicolson method for solving PDEs to other known methods or seek to improve upon it. The Crank-Nicolson scheme has proved well suited for this particular problem but may not be applicable to all variations of PDEs.

## V. CONCLUSION

In this report we have looked at the two-dimensional Schrödinger equation, and used it to describe the time-evolution of a wave function describing a single particle passing through one, two and three slits in a two-dimensional closed box. The time evolution of the Schrödinger equation was solved using the Crank-Nicolson scheme for partial differential equations. Looking at the probability distribution along the  $y$ -axis for a given  $x$  and  $t$ , we found the expected interference pattern of the probability distribution of the particle's position. Together with our 2D-visualisations of the system and an evaluation of conserved quantities, we can conclude that the Crank-Nicolson scheme is well suited for solving PDEs similar to the Schrödinger equation. We looked at the deviation of the total probability  $p - 1$  of the Crank-Nicolson scheme and found the deviation to be of magnitude  $10^{-15}$ . This deviation is likely due to the numerical precision of the computer, and so the resulting simulations are reliable.

- 
- [1] O. Donati, G. P. Missiroli, and G. Pozzi, *American Journal of Physics* **41**, 639 (1973), <https://doi.org/10.1119/1.1987321>.
  - [2] E. Schrödinger, *Physical Review* **28** (1926).
  - [3] "The nobel prize in physics 1933," Available at <https://www.nobelprize.org/prizes/physics/1933/summary/> December 9, 2022.
  - [4] J. Crank and P. Nicolson, *Mathematical Proceedings of the Cambridge Philosophical Society* **43**, 50–67 (1947).
  - [5] IBM, "Floating-point formats," Available at <https://www.ibm.com/docs/no/xl-c-and-cpp-linux/16.1.0?topic=operations-floating-point-formats> December 9, 2022.

### Appendix A: Deriving the discretized Schrodinger equation using the Crank-Nicolson scheme

The unitless schrodinger equation is

$$i \frac{\partial u}{\partial t} = F(x, y, t),$$

where  $F(x, y, t) = -\frac{\partial^2 u}{\partial x^2} - \frac{\partial^2 u}{\partial y^2} + v(x, y)u$ . We can find the second derivatives with respect to both  $x$  and  $y$  numerically as

$$\frac{\partial^2 u}{\partial x^2} = \frac{u_{i+1,j}^n - 2u_{ij}^n + u_{i-1,j}^n}{\Delta x^2},$$

and

$$\frac{\partial^2 u}{\partial y^2} = \frac{u_{i,j+1}^n - 2u_{ij}^n + u_{i,j-1}^n}{\Delta y^2}.$$

Using this, together with the discretized potential  $v_{ij}$ , we have that

$$F_{ij}^n = -\frac{u_{i+1,j}^n - 2u_{ij}^n + u_{i-1,j}^n}{\Delta x^2} - \frac{u_{i,j+1}^n - 2u_{ij}^n + u_{i,j-1}^n}{\Delta y^2} + v_{ij}u_{ij}^n.$$

Furthermore, we have that the Crank-Nicolson form of the Schrodinger equation is

$$i \frac{u_{ij}^{n+1} - u_{ij}^n}{\Delta t} = \frac{1}{2}(F_{ij}^n + F_{ij}^{n+1}).$$

We insert the expressions for  $F_{ij}^n$ , and use that  $\Delta x = \Delta y = h$ . Our equation then becomes:

$$\begin{aligned} i \frac{u_{ij}^{n+1} - u_{ij}^n}{\Delta t} &= \frac{1}{2} \left[ -\frac{u_{i+1,j}^n - 2u_{ij}^n + u_{i-1,j}^n}{h^2} - \frac{u_{i,j+1}^n - 2u_{ij}^n + u_{i,j-1}^n}{h^2} + v_{ij}u_{ij}^n \right. \\ &\quad \left. - \frac{u_{i+1,j}^{n+1} - 2u_{ij}^{n+1} + u_{i-1,j}^{n+1}}{h^2} - \frac{u_{i,j+1}^{n+1} - 2u_{ij}^{n+1} + u_{i,j-1}^{n+1}}{h^2} + v_{ij}u_{ij}^{n+1} \right] \\ u_{ij}^{n+1} - u_{ij}^n &= -\frac{\Delta t}{2ih^2} [u_{i+1,j}^n - 2u_{ij}^n + u_{i-1,j}^n + u_{i,j+1}^n - 2u_{ij}^n + u_{i,j-1}^n - h^2 v_{ij}u_{ij}^n \\ &\quad + u_{i+1,j}^{n+1} - 2u_{ij}^{n+1} + u_{i-1,j}^{n+1} + u_{i,j+1}^{n+1} - 2u_{ij}^{n+1} + u_{i,j-1}^{n+1} - h^2 v_{ij}u_{ij}^{n+1}] \\ u_{ij}^{n+1} - u_{ij}^n &= \frac{i\Delta t}{2h^2} [u_{i+1,j}^n - 2u_{ij}^n + u_{i-1,j}^n + u_{i,j+1}^n - 2u_{ij}^n + u_{i,j-1}^n - h^2 v_{ij}u_{ij}^n \\ &\quad + u_{i+1,j}^{n+1} - 2u_{ij}^{n+1} + u_{i-1,j}^{n+1} + u_{i,j+1}^{n+1} - 2u_{ij}^{n+1} + u_{i,j-1}^{n+1} - h^2 v_{ij}u_{ij}^{n+1}]. \end{aligned}$$

We can then move all the  $n+1$  terms to the left side of the equation, and all the  $n$  terms to the right side, giving us

$$\begin{aligned} u_{ij}^{n+1} - \frac{i\Delta t}{2h^2} [u_{i+1,j}^{n+1} - 2u_{ij}^{n+1} + u_{i-1,j}^{n+1}] - \frac{i\Delta t}{2h^2} [u_{i,j+1}^{n+1} - 2u_{ij}^{n+1} + u_{i,j-1}^{n+1}] + \frac{i\Delta t}{2} v_{ij}u_{ij}^{n+1} \\ = u_{ij}^n + \frac{i\Delta t}{2h^2} [u_{i+1,j}^n - 2u_{ij}^n + u_{i-1,j}^n] + \frac{i\Delta t}{2h^2} [u_{i,j+1}^n - 2u_{ij}^n + u_{i,j-1}^n] - \frac{i\Delta t}{2} v_{ij}u_{ij}^n \\ u_{ij}^{n+1} - r [u_{i+1,j}^{n+1} - 2u_{ij}^{n+1} + u_{i-1,j}^{n+1}] - r [u_{i,j+1}^{n+1} - 2u_{ij}^{n+1} + u_{i,j-1}^{n+1}] + \frac{i\Delta t}{2} v_{ij}u_{ij}^{n+1} \\ = u_{ij}^n + r [u_{i+1,j}^n - 2u_{ij}^n + u_{i-1,j}^n] + r [u_{i,j+1}^n - 2u_{ij}^n + u_{i,j-1}^n] - \frac{i\Delta t}{2} v_{ij}u_{ij}^n, \end{aligned}$$

where  $r \equiv \frac{i\Delta t}{2h^2}$ .